

QtAC: An R-package for analyzing complex systems development in the framework of the adaptive cycle metaphor

Hannah Schrenk ^{a,*}, Carlos Garcia-Perez ^a, Nico Schreiber ^a, Wolfgang zu Castell ^{a,b}

^a Strategy & Digitalization, Helmholtz Zentrum München, Ingolstädter Landstraße 1, D-85764 Neuherberg, Germany

^b Department Geoinformation, Helmholtz Zentrum Potsdam, Deutsches GeoForschungsZentrum GFZ, Telegrafenberg, 14473 Potsdam, Germany

ARTICLE INFO

Keywords:

Complex systems
Adaptive cycle
Information networks
R package
Biodiversity

ABSTRACT

We present the QtAC R-package, which enables the analysis and assessment of general complex systems in terms of the adaptive cycle metaphor. According to the metaphor, complex systems typically develop through alternating phases of consolidation and reorganization, being defined by the systemic properties of potential, connectedness, and resilience. QtAC builds on a recently published universal method of quantifying the adaptive cycle. Based on time series of abundance data, networks of information transfer are estimated, yielding insight into the internal interaction structure of the system and the functional role of its components. Potential, connectedness, and resilience are computed on basis of the information networks, defining the system's course through the cycle. We illustrate the application of QtAC via an exemplary case study on grassland communities.

1. Software and data availability statement

The QtAC R-package is available through the GitHub repository (Schrenk et al., 2020b) under the MIT License. It was first released in August 2020. The code runs on Windows and Linux operating systems with R version 3.6 or higher. All data used in this article is provided as supplementary material of the paper and through the GitHub repository.

2. Introduction

Understanding complex systems remains one of the most challenging endeavors in many scientific disciplines, ranging from ecology, over economy, to social sciences. A particular difficulty lies in the fact that emerging system-wide phenomena need to be connected with the specific functional role of single components to get a concise picture. An established qualitative framework for the assessment of complex systems is provided by the adaptive cycle metaphor. It was originally introduced in ecological context by Holling in 1986 (Holling, 1986) and taken up in a more general form in the course of Gunderson's and Holling's panarchy concept in the early 2000s (Gunderson and Holling, 2002). The metaphor describes complex systems development as alternation of phases of growth, consolidation and predictability, with phases of release, reorganization and stochasticity. Recently, a generally applicable method to quantify the adaptive cycle on basis of abundance data has been published by zu Castell and Schrenk (2020). In contrast to previously published methods of quantifying the adaptive

cycle (e.g. Beier et al. (2009), Pelling and Manuel-Navarrete (2011) and Angeler et al. (2016)), it is independent of the concrete instantiation of the underlying system. In this article, we present the QtAC R-package, which allows a straightforward application of this method.

According to the adaptive cycle metaphor, the development of complex systems is shaped by three systemic properties: the system's potential to react to future changes, the connectedness among its components, and the system's resilience capturing the ability of the system to counteract unexpected perturbations. Phases of growth and consolidation are characterized by an increase in potential and connectedness at the cost of resilience. Sudden decreases in connectedness and potential accompanied by sudden increases in resilience mark the beginning of phases of release and reorganization. This interplay allows a complex system to repeatedly adapt to a changing environment in balancing stability and adaptability. The method presented by zu Castell and Schrenk provides a way to estimate the course of a system through the adaptive cycle for arbitrary complex systems. It has been applied to both real and simulated data (zu Castell and Schrenk, 2020; Schrenk et al., 2021).

The method consists of two main steps. In the first step, pairwise transfer entropy as being defined in Schreiber (2000) is estimated on basis of time series of abundance data. Considering the system's components as nodes and the transfer entropy as edges, this step yields a directed, weighted network capturing a model of the system's interaction structure. In the second step, potential, connectedness, and

* Corresponding author.

E-mail address: hannah.schrenk@helmholtz-muenchen.de (H. Schrenk).

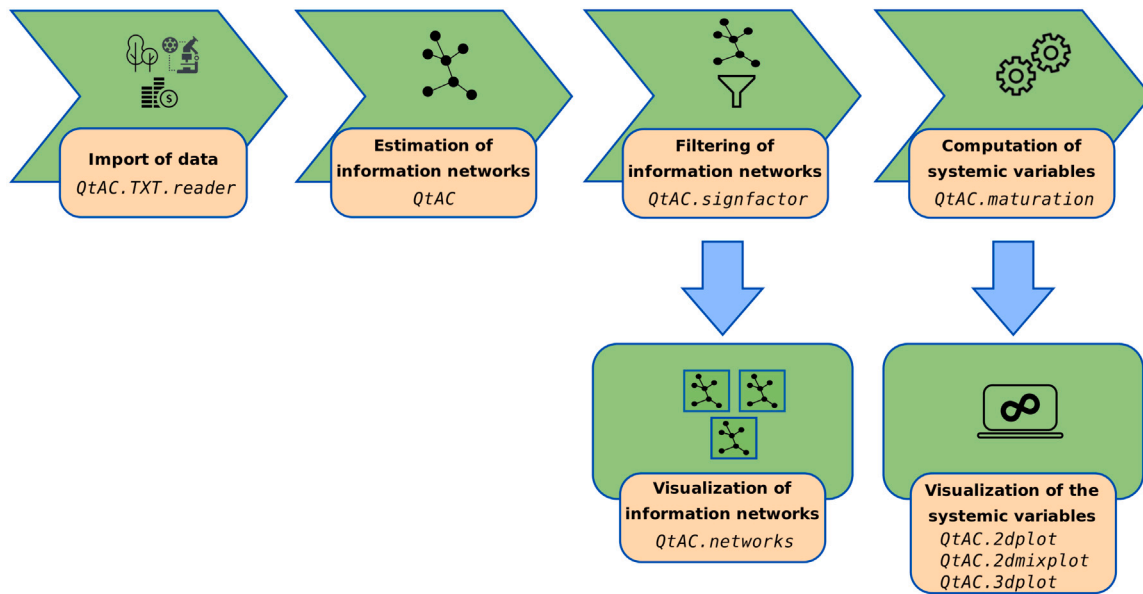


Fig. 1. Workflow of the R-package QtAC.

resilience are computed on basis of the inferred information network. Here, the definitions of potential and connectedness are inspired by notions introduced by Ulanowicz in the course of his ascendancy theory (see e.g. Ulanowicz et al. (2009)). A variant of the common spectral graph theoretical notion of connectivity (see e.g. Chung (1997)) is used to measure resilience.

By shifting the time frame serving as basis for the estimation of transfer entropy in the first step, a series of networks and thereby of the three systemic variables can be determined. With the latter allowing to assess system-wide behavior and the networks giving insights into the role of single components, the method provides a holistic approach for the analysis of complex systems. So far, case studies on ecological, economic, and microbiological systems have been conducted in zu Castell and Schrenk (2020) and Schrenk et al. (2020a, 2021).

The R-package QtAC (Quantifying the Adaptive Cycle) makes the method accessible to the scientific community. The functions included in the package allow for a straightforward import of the data, estimation of information networks, and computation of the systemic variables. The information theoretic estimations are based on functions provided by the JIDT toolkit (Lizier, 2014). Via various parameters, the user can adjust the estimation to the system properties and the underlying question. QtAC offers two- and three-dimensional visualization of the results.

At first, we present the QtAC workflow, including a description of its main functions. Subsequently, we illustrate the application of the method and common follow-up analyses using an example of grassland communities of varying species and functional richness. The underlying data was collected in course of the Jena Experiment (Weisser et al., 2017), a long-term biodiversity experiment. Possibilities and limits of system and parameter choice are discussed in the course of this case study. We conclude with a short outlook on planned enhancements of the package.

3. QtAC workflow

As schematically displayed in Fig. 1, QtAC offers a simple and clear workflow, which is organized around the two main steps of the underlying method (see zu Castell and Schrenk (2020) for details). In the following, we will present the workflow in more detail.

3.1. Input data

In order to conduct a system analysis with QtAC, the user needs to provide time series of *abundance data*. By abundance data, we denote any kind of data reflecting the strength of a component and capturing the success or failure resulting from its interactions. The term *abundance* therefore is used in a more general sense. In an ecosystem, abundance of species could for example be quantified via biomass or the number of individuals. In an economic system, the capital or the number of employees may quantify abundances of a company. Note that both type of components and unit of abundances may differ from each other within the observed system. Since QtAC estimates the degree of randomness in time series data, the approach is independent of the concrete instantiation of the time series. Hence, an ecosystem could for example include animal species, quantified by their number of individuals, and plant species, quantified by their respective biomass. However, QtAC relies on equidistantly sampled time series. If this is not the case, this property can be achieved by a preceding interpolation step. Besides, time series need to have a length of at least five time points, since otherwise, a reliable statistical estimation is not feasible. As for the overall lengths of the time series, the package can easily deal with longer series. Obviously, longer series lead to increased computing effort. Also interpretability of the results depends on enough data being available.

3.2. Estimating and visualizing information dynamics

The main function QtAC allows the user to extract information dynamics from time series data. By information dynamics, we denote the temporal change of the network of pairwise information transfer resulting from effective interactions among the system's components.

Let (a_1, \dots, a_n) and (b_1, \dots, b_n) denote the time series of abundance data of two components A and B , respectively. Following the methodology described in zu Castell and Schrenk (2020), directed information transfer $T_{B \rightarrow A}$ from B to A at time point t is determined on basis of their abundance data within a preceding time window (a_{t-w+1}, \dots, a_t) and (b_{t-w+1}, \dots, b_t) , respectively. The size w of this time window is user-defined. Note that the choice of this and all further parameters requires a certain background-knowledge of the observed system. Optionally, some of the parameters can be estimated using appropriate optimization methods (see e.g. Lizier (2014)). Sensitivity analyses should be conducted to study the impact of the parameter choices.

In QtAC, information transfer is quantified by the established measure of *transfer entropy* (Schreiber, 2000). It is estimated by means of the Kraskov–Stögbauer–Grassberger estimator as being incorporated in the JIDT toolkit (Lizier, 2014). Various customizable parameters are inherited from this toolkit. The estimator is based on the principles of a simple kernel estimator and is optimized to deal with small sample sizes; see Kaiser and Schreiber (2002) and Kraskov et al. (2004) for details. This procedure is repeated for every ordered pair of components and every time point $w \leq t \leq n$.

Note that, if the length of the timeseries is below 15, two additional data points are interpolated between each pair of data points (a_i, a_{i+1}) by means of a piecewise cubic spline before the estimation, thereby increasing stability of the results. The spline function is computed using the R-package *pracma* (Borchers, 2019).

QtAC conducts a significance test as part of the estimations. This bootstrapping test is part of the JIDT toolkit (Lizier, 2014). The function `QtAC.signfactor` allows the user to filter the results of QtAC with respect to their significance before further processing.

Using the function `QtAC.networks`, the user can visualize the estimated information dynamics in form of a series of directed, weighted networks, the nodes of which represent the system’s components and the edges of which represent the respective information transfer. The visualization function is based on the R-package *igraph* and offers various layout options inherited from this package (Csardi and Nepusz, 2006).

3.3. Computing and visualizing the systemic variables

Following the method by zu Castell and Schrenk (2020), potential, connectedness and resilience are defined as properties of the system’s information network at the respective time. Consider the directed, weighted network G of information transfers e among the system’s components \mathcal{V} at time point t , i.e.

$$G = (\mathcal{V}, \{e_{B \rightarrow A} | (B, A) \in \mathcal{V} \times \mathcal{V}\})$$

with weight function

$$\omega : \mathcal{V} \times \mathcal{V} \rightarrow \mathbb{R}_{\geq 0}$$

$$e_{B \rightarrow A} \mapsto T_{B \rightarrow A}.$$

Then, the system’s *potential* at the given time is defined as

$$P = - \sum_{(Y,X) \in \mathcal{V} \times \mathcal{V}} T_{Y \rightarrow X} \cdot \log_2 \left(\frac{T_{Y \rightarrow X}}{T} \right)$$

and the system’s *connectedness* as

$$C = \sum_{(Y,X) \in \mathcal{V} \times \mathcal{V}} T_{Y \rightarrow X} \cdot \log_2 \left(\frac{T_{Y \rightarrow X} \cdot T}{\sum_{X' \in \mathcal{V}} T_{Y \rightarrow X'} \cdot \sum_{Y' \in \mathcal{V}} T_{Y' \rightarrow X}} \right),$$

where

$$T = \sum_{(Y,X) \in \mathcal{V} \times \mathcal{V}} T_{Y \rightarrow X}.$$

The two definitions are inspired by the information theoretical measures of capacity and ascendancy, which were originally introduced by Ulanowicz et al. (2009).

The definition of resilience given by zu Castell and Schrenk (2020) is the directed analog to the established spectral graph theoretical measure of connectivity (see e.g. Chung (1997)). With A denoting the adjacency matrix of G , D_{out} and D_{in} its directed degree matrices, and $c > 0$ a standardization constant, the graph’s directed Laplacian matrices are given as

$$L_{out} = c \cdot D_{out}^{-\frac{1}{2}} (D_{out} - A) \quad \text{and} \quad L_{in} = c \cdot (D_{in} - A) D_{in}^{-\frac{1}{2}}.$$

Then, resilience is defined as the smallest real part of the non-trivial eigenvalues of L_{out} and L_{in} , i.e.

$$R = \min \{ \Re \sigma : \sigma \in \text{Spec}(L_{out}) \cup \text{Spec}(L_{in}), \sigma \neq 0 \}.$$

In QtAC, the computation of the systemic variables on basis of a series of information networks is performed by the function `QtAC.maturation`. Here, the user can choose between different standardization constants c . Especially when comparing different systems, standardization can prove useful. In order to choose a suitable value, the user should answer questions like ‘Should resilience in this case depend on the absolute edge weights of the information network G ? Consequently, should a complete network with uniform edge weight 2 be more resilient than a complete network with uniform edge weight 1?’ or ‘Should the resilience depend on the number of nodes of G ? Hence, should a complete network on 10 nodes be more resilient than a complete network on 5 nodes?’. There are no generally applicable answers to these questions. They depend on the specific research question and the context to be studied only. The inherent relative nature of the notion of resilience has been frequently discussed (compare e.g. Allen et al. (2018)). Let M denote the maximal edge weight of G . Then, QtAC provides non-trivial standardization with respect to the number of nodes of G via

$$c = \frac{\sqrt{N-1}}{N},$$

with respect to the maximal edge weight of G via

$$c = \frac{1}{\sqrt{M}},$$

or with respect to both via

$$c = \frac{\sqrt{N-1}}{N \cdot \sqrt{M}}.$$

The function returns a series of the three systemic variables, defining the system’s course through the adaptive cycle in the respective time period.

QtAC offers various possibilities to visualize the development of the systemic variables. Via `QtAC.2dplot`, the variables can be plotted separately against time. The function `QtAC.2dmixplot` returns two-dimensional plots as well with two variables plotted against each other. In order to visualize the development of the variables in the typical layout of the adaptive cycle metaphor, QtAC provides the function `QtAC.3dplot`. It is based on the R-package *rgl* (Adler et al., 2019) and returns a three-dimensional plot of the variables, which can be rotated and thereby examined from different angles. In all cases, a curve through the data points is computed via a piecewise cubic smoothing spline, which is inherited from the R-package *pracma* (Borchers, 2019).

4. Use case: Exploring grassland communities

We illustrate the application of QtAC by means of an exemplary test case of grassland communities. The data underlying this test case stems from the Jena Experiment, a grassland biodiversity experiment located near Jena, Germany (see Weisser et al. (2017)). Within the last years, a multitude of studies has been performed on basis of data gained in the experiment, covering biodiversity effects on aboveground productivity (Marquard et al., 2013), diversity–stability relationships (Roscher et al., 2011), and effects of management intensity on grassland resistance (Vogel et al., 2012).

In the course of the main experiment, 82 plots of 20 m × 20 m were set up on former arable land in 2002. Mixtures of 1, 2, 4, 8, 16, and 60 regional grassland species were established in these plots. The species had been assigned to four functional groups in advance, namely grasses, small herbs, tall herbs, and legume species. The composition of species in each plot was determined randomly with constraints to ensure all possible combinations of species number and number of functional groups. Twice a year, the plots were mown and non-sown species were weeded. Aside from that, no further treatments took place. See Jena Experiment (2002) for a description of the main experiment, including a list of all 60 species and their respective functional group.

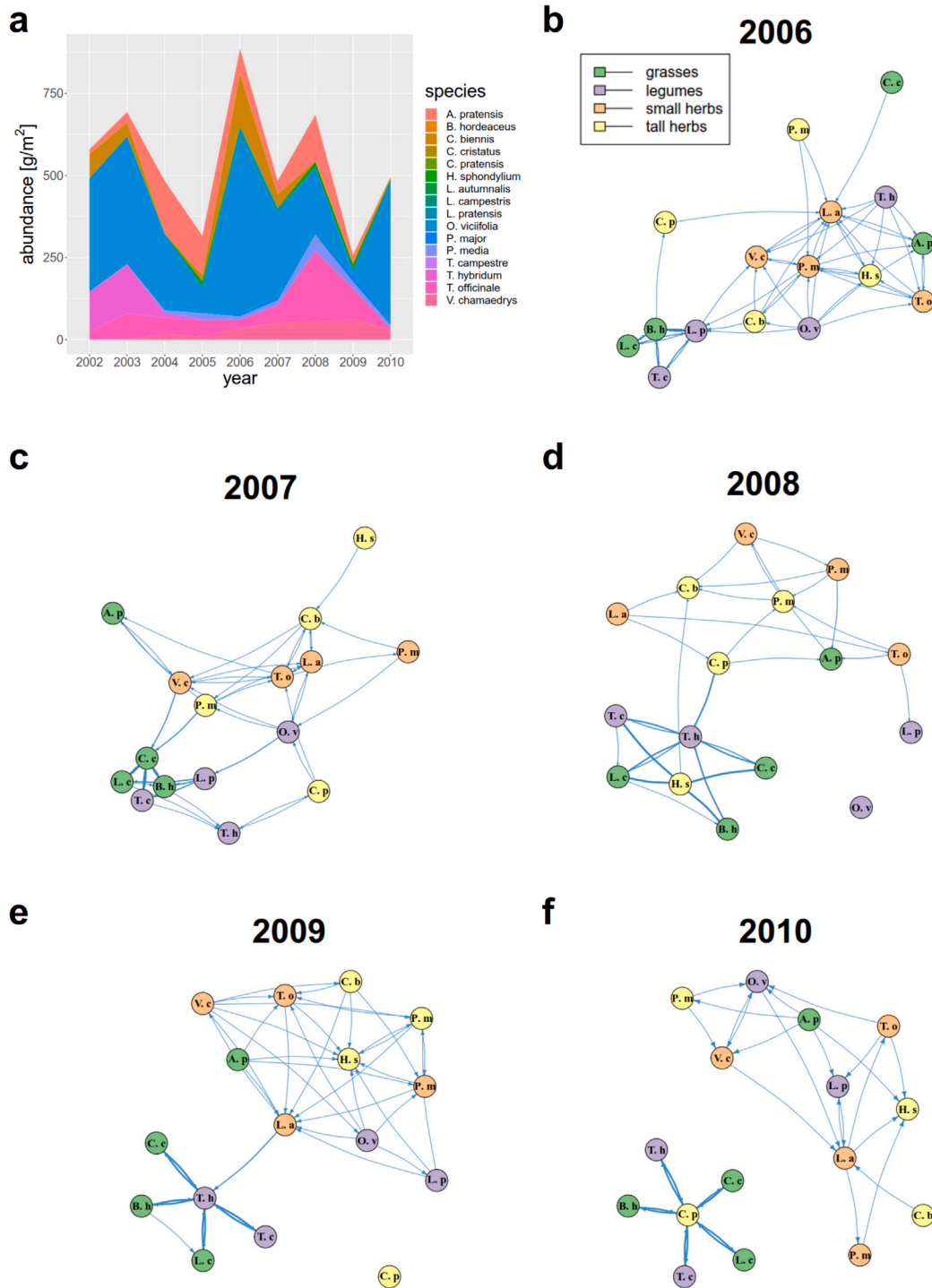


Fig. 2. Information theoretic analysis of the plant community in plot B4A18. (a) Abundances (in dry weight) of the 16 sown species between 2002 and 2010. (b)–(f) Networks of information transfer estimated on basis of the abundances displayed in (a). The nodes are colored according to the functional group of the respective species.

In the following case study, we investigate and compare the systematic development of the 34 communities of at least 8 species. Our analysis is based on species-specific biomass data collected once a year from 2002 to 2010 in June prior to the first mowing (Weigelt et al., 2016). We provide the data and code underlying the following figures with this article (Data_casestudies.7z, Results_casestudies.7z and Code_casestudies.md).

We want to demonstrate the exploration of a single plant system, namely the community in plot B4A18, in which 16 species of four different functional groups were sown. The data is part of Weigelt et al.

(2016). We recommend to always inspect the time series data before starting the analysis to get a first impression of the system at hand (see Fig. 2(a)).

In order to gain an insight into the information dynamics, we want to study the development of the system's information network. Recall that the network at a given time point is estimated on basis of a window of a fixed length of preceding abundance data. Thereby, every network reflects a temporally more local, rather than the global, information structure of the system. By shifting the window along the time series, the development of the information structure can be captured. With

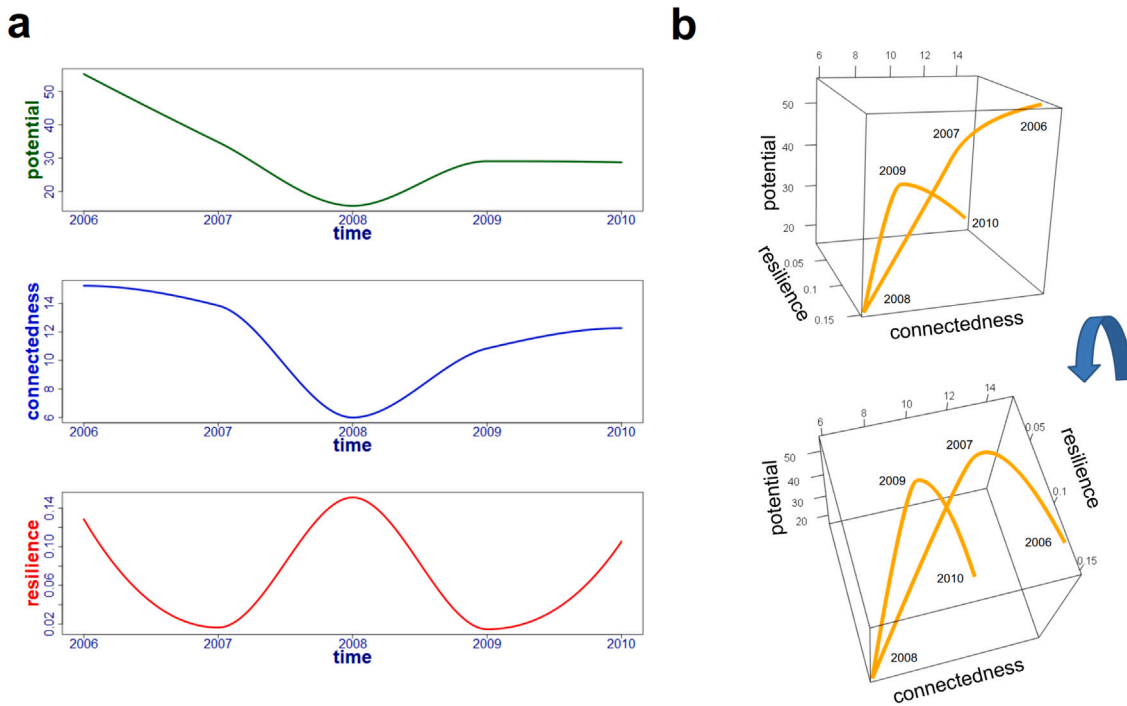


Fig. 3. Development of the three systemic variables in plot B4A18 between 2006 and 2010. (a) Potential, connectedness, and resilience of the plant community. (b) Three-dimensional plot of potential, connectedness, and resilience from two different perspectives.

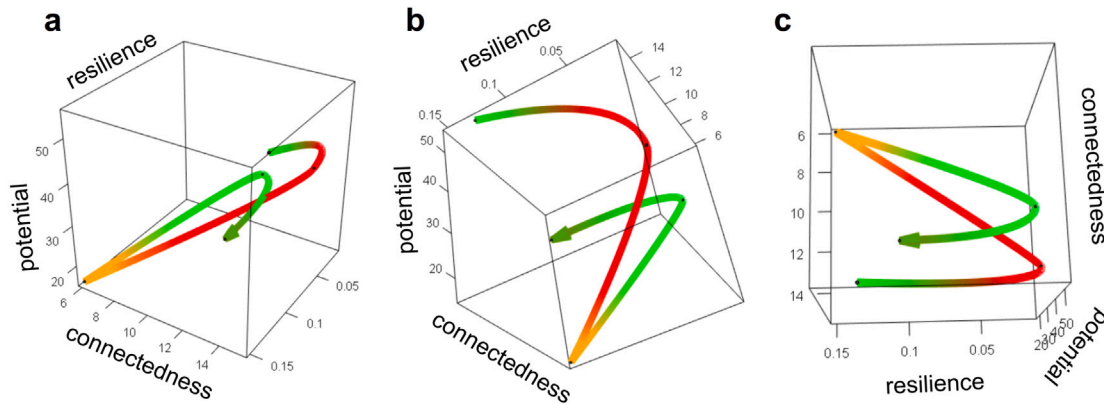


Fig. 4. Three-dimensional plot of potential, connectedness, and resilience of plot B4A18 between 2006 and 2010 from three perspectives. The phases are displayed in color.

the window size determining the time point of the earliest network estimated, a larger window size generally leads to a shorter analysis period. The choice of this parameter is always a trade-off between statistical stability provided by large window sizes and a more precise temporal resolution gained by small window sizes. QtAC generally does not accept window sizes below five in order to guarantee statistical reliability of the results.

In order to extract and follow the strong dynamics in abundance data of plot B4A18 (Fig. 2(a)), we need the analysis period to start as early as possible. Hence, we choose a window size of $w = 5$ years, allowing us to analyze the system’s information structure from 2006 on.

Crucial parameters for estimating transfer entropy are the (time- and species-independent) embedding length of source $l \leq w$ and destination past history $k \leq w$ (see Schreiber (2000)). They should be chosen in a way such that, knowing the past l states of the source variable, no further relevant information about its next state is gained by extending to more than l states. The same applies for k and the destination variable. Due to computational reasons, $k=l=1$ is a common choice.

However, choosing k too small, information being contained in the past of the destination variable may be erroneously considered as information transfer from the source variable. Equally, choosing l too large, information transfer might be over-estimated as well. On the other hand, choosing l too small or k too large, an existing information transfer might not be recognized (compare e.g. Lizier (2014)). In the absence of sufficient background knowledge of the system components, one can estimate the embedding lengths using for example the Ragwitz optimization method as provided with the JIDT toolkit (Lizier, 2014).

Recall that, in the case of a window size below 15, two additional data points are interpolated between each pair of successive data points. Hence, one originally preceding data point corresponds to three interpolated preceding data points. The user should be aware of this fact when choosing the history lengths. In the case of community B4A18, we choose a history length of four, corresponding to almost one and a half years in reality. A sensitivity analysis shows that our results are robust with respect to both a slightly lower and slightly higher history length (compare Fig. A.1).

We choose a comparably low level of random Gaussian noise added in the estimation, namely $1e-30$. A certain amount of noise is required

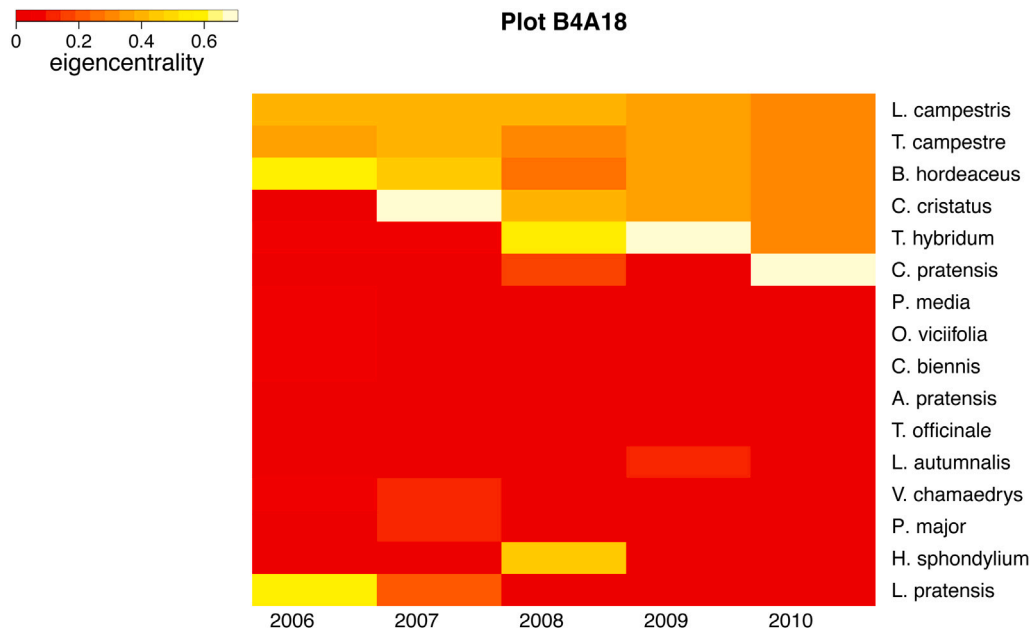


Fig. 5. Heatmap displaying the eigencentralities of the components of community B4A18 in its information network between 2006 and 2010.

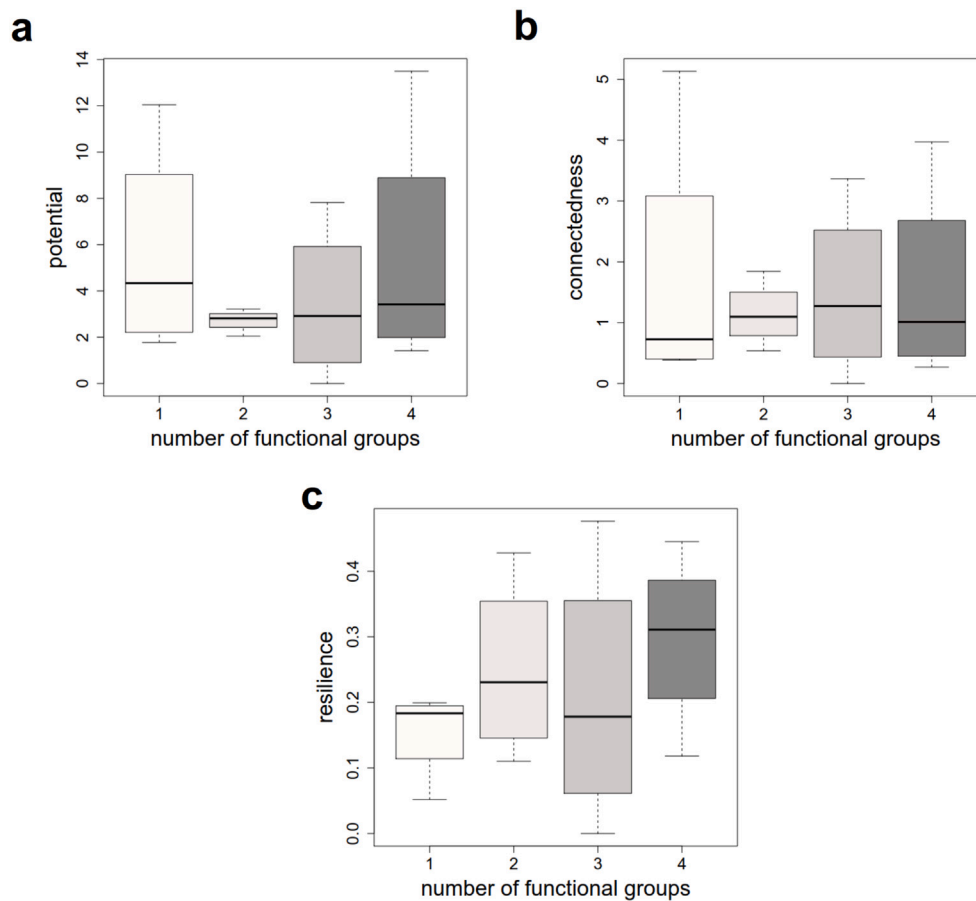


Fig. 6. Boxplots showing (a) potential (b) connectedness and (c) resilience of the eight-species-communities. The variables are computed on basis of their respective information networks in 2010 and grouped according to their degree of functional diversity.

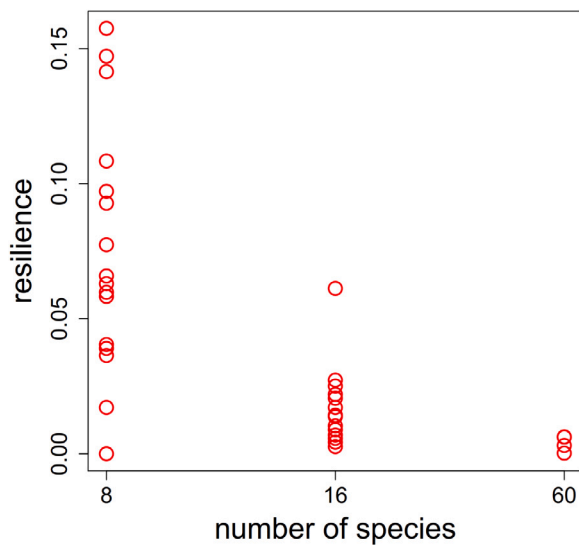


Fig. 7. Resilience of each plant community computed on basis of their respective information networks in 2010 and grouped with respect to the number of species sown in the respective plot.

to guarantee the functioning of the estimator (see Kraskov (2008)). However, especially in the case of short time series, high noise levels can lead to very unstable results. Our choice is based on a sensitivity analysis conducted in advance. Fig. A.2 displays the mean and standard deviation of the systemic variables for different levels of noise added and 20 computations each. Clearly, potential is robust across all levels of random noise. Connectedness shows to be robust for all noise levels except for $1e-08$ (A.2(a)). Note that this is the default value of random noise in the JIDT package. Resilience shows a high standard deviation across all noise levels. This is due to the fact that resilience, in contrast to potential and connectedness, is a *local* measure, being highly sensitive to the existence or non-existence of single edges in the underlying information network. Using a noise level of $1e-30$, the only value showing a remarkably high standard deviation is the resilience in 2008. Before analyzing a specific information network in detail, the user should compare the networks of different runs to get a better understanding of what edges might lead to jumps in resilience. The respective information transfers should be interpreted with care.

Based on the chosen parameters, the function QtAC returns adjacency and significance matrices for every year between 2006 and 2010. We filter the results using a significance level of 0.1. In this specific case, lower significance levels lead to consistently very sparse adjacency matrices, suggesting that structuring information transfer was lost in the process of filtering. Fig. A.3 shows the systemic variables for lower significance levels. It can be clearly seen that the results are robust down to a significance level of 0.05. In order to assure reliable results, we recommend not to use a significance level above 0.1. The (filtered) networks are plotted by means of QtAC.network. Using layout nicely, nodes' positions reflect their network theoretic relation to each other, thereby enabling an impression of the overall development of the network at first sight (see Fig. 2(b–f)). Nodes are colored according to the functional group of the respective species.

Considering the development of the information network we observe an interesting pattern. In 2006, there already is a subcommunity of closely connectedness nodes, including *B. horadecus*, *T. campestris*, and *L. campestris*. Throughout the following year, connectivity within the subcommunity increases, while starting from 2008, it more and more separates from the rest of the network. In 2010, the network eventually splits into two components, one being the subcommunity including three further species, namely *C. cristatus*, *T. hybridum*, *C. pratensis*. This subcommunity takes a central position in the overall

network. Except for *C. pratensis*, the community consists of grasses and legumes, only.

From the point of view of the adaptive cycle, the sudden and relatively strong structural change in the network from 2007 to 2008 can hint towards the transition to a new cycle. From 2008 on, the new structure intensifies, showing in an increasing separation of the subcommunity. Besides, the internal organization and connectivity in both subcommunities increases. Such directed development usually indicates an *r/K*-phase.

The development of the three systemic variables, computed via QtAC.maturatation and visualized via QtAC.2dplot (Fig. 3(a)) and QtAC.3dplot (Fig. 3(b)) confirm our first impression. Connectedness and potential are comparably high in 2006. While potential already decreases, connectedness remains almost constant during the first year. Resilience strongly decreases. This pattern suggests a late *K*-phase. From 2007 to 2008, connectedness strongly decreases while resilience strongly increases, indicating a classical Ω -phase. The Ω -phase coincides with the onset of the separation of the subcommunity. Besides, the rest of the network seems to be more loosely connected. From 2008 to 2009, connectedness and potential increase, while resilience decreases. This behavior is characteristic of an *r*-phase. From 2009 on, the increase in potential and connectedness continues, however more slowly, suggesting that the system has entered the early *K*-phase. Atypically, resilience increases during this year. Considering the networks, this phenomenon can be traced back to the disappearance of the edge between *T. hybridum* and *L. autumnalis*.

The three-dimensional graphs in Fig. 4 have been colored according to the typical color scheme of the adaptive cycle's phases.

A helpful visualization tool for information networks are heatmaps showing eigencentralities of the nodes. Eigencentrality measures a node's degree of connection within the network as being interpreted as communication network (see Csardi and Nepusz (2006)). It thus to some degree indicates importance of a node for the system as a whole. The heatmap of the community in plot B4A18 (Fig. 5) clearly reflects the gradual emergence of the subcommunity. Especially for large systems, such a heatmap can help to gain an overview of the network's topology and the position of single components within the network. For example, compare the case study on a prairie-forest ecotone in zu Castell and Schrenk (2020).

Following previous publications on the Jena Experiment (see e.g. Vogel et al. (2012)), we want to compare resilience (as well as potential and connectedness) of different plots, thereby gaining insight into the relation of each of these properties to community size and composition. At first, we restrict ourselves to the 16 communities of eight species, grouped according to the functional diversity of their respective plant community. We compute potential, connectedness, and resilience of each community on basis of their information network in 2010. Fig. 6 visualizes the results in form of a boxplot. Note that each of the four groups of functional diversity contains exactly four communities. Fig. 6(c) shows that the median of resilience is maximal for communities consisting of four functional groups. This matches earlier results: In Allan et al. (2011), it was shown that the level of functioning is higher in more diverse communities, due to turnover of functionally complementary species.

Figs. 6(a)–(b) display the results for potential and connectedness. In both cases, we cannot observe the results as clear patterns as in the case of resilience. Of course, with only four communities existing for each degree of functional diversity, the number of samples is rather small. It would be interesting to conduct the analysis with a higher number of samples.

In order to investigate the relation between resilience and species richness, we compute the resilience of all 34 communities in 2010. Per default, resilience of a network is standardized with respect to the maximal information transfer occurring in the network, yielding a certain comparability across time points. Here, using `res_stand = "maxweightnodes"`, we standardize not only with respect to maximal

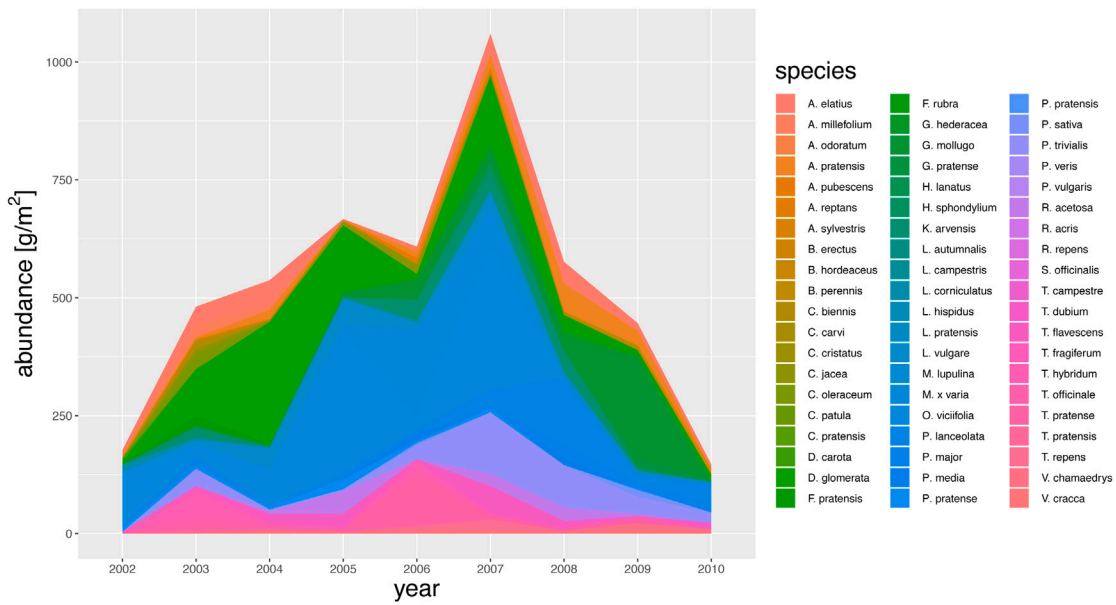


Fig. 8. Development of the abundances of the 60 species in plot B1A22 between 2002 and 2010.

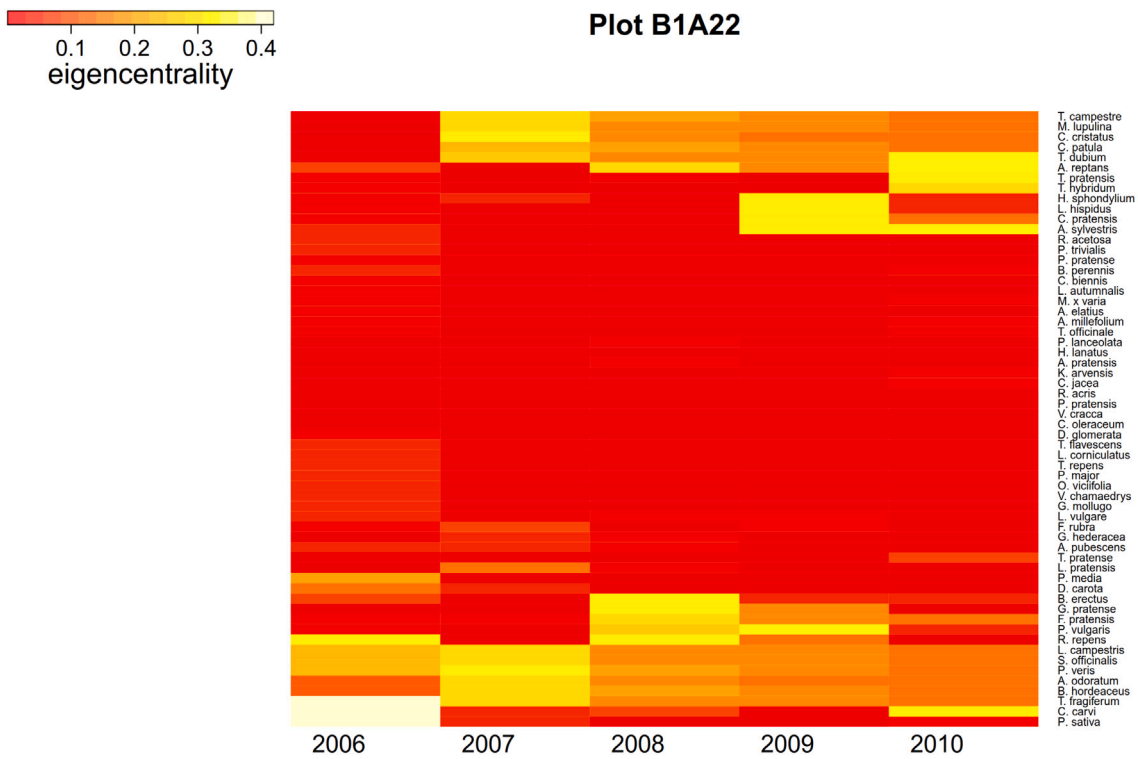


Fig. 9. Heatmap showing the eigencentality of the 60 species of plot B1A22 on basis of the estimated networks of information transfer between 2006 and 2010.

edge weight but with respect to the number of nodes as well. We visualize the results in form of a scatterplot to make clear that the sizes of the groups strongly vary. Note that, in previous publications on the Jena Experiment, the common expectation of resilience increasing with species richness could only be confirmed under high treatment intensity. However, such treatment was not applied in the main experiment (see Vogel et al. (2012)). Accordingly, Fig. 7 shows that variance and mean resilience clearly decrease with increasing species richness.

Being generally of wide interest, the results of our small exemplary case study could serve as starting point for comprehensive, large-scale studies on the relation between resilience, functional diversity, and species richness in plant communities.

We continue with the application of QtAC to one of the large communities, namely the community in plot B1A22, consisting of 60 species. Again, we get a quick overview of the system by means of the development of the components' abundances (Fig. 8).

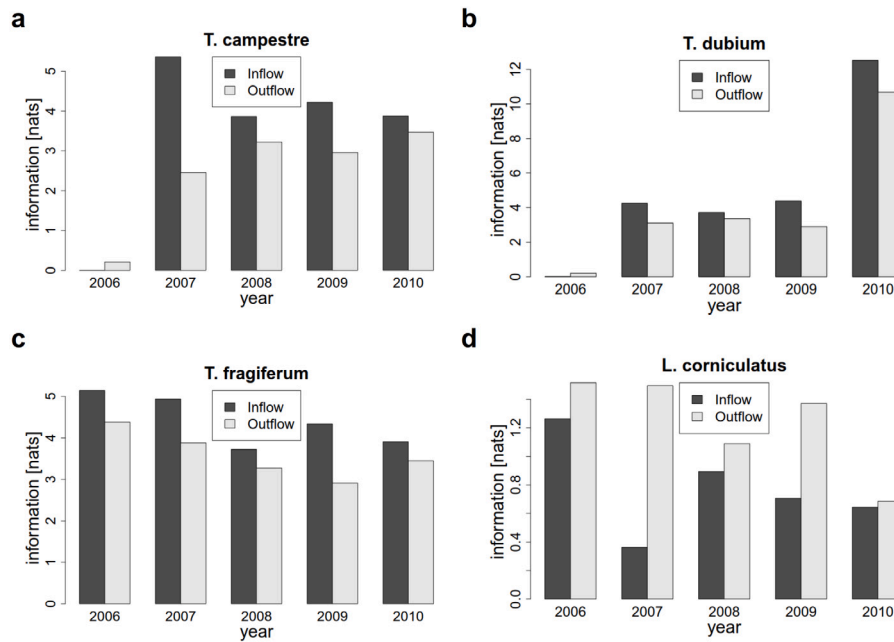


Fig. 10. Total information in- and outflow of (a) *T. campestre*, (b) *T. dubium*, (c) *T. fragiferum*, and (d) *L. corniculatus* in the information networks of plot B1A22 between 2006 and 2010.

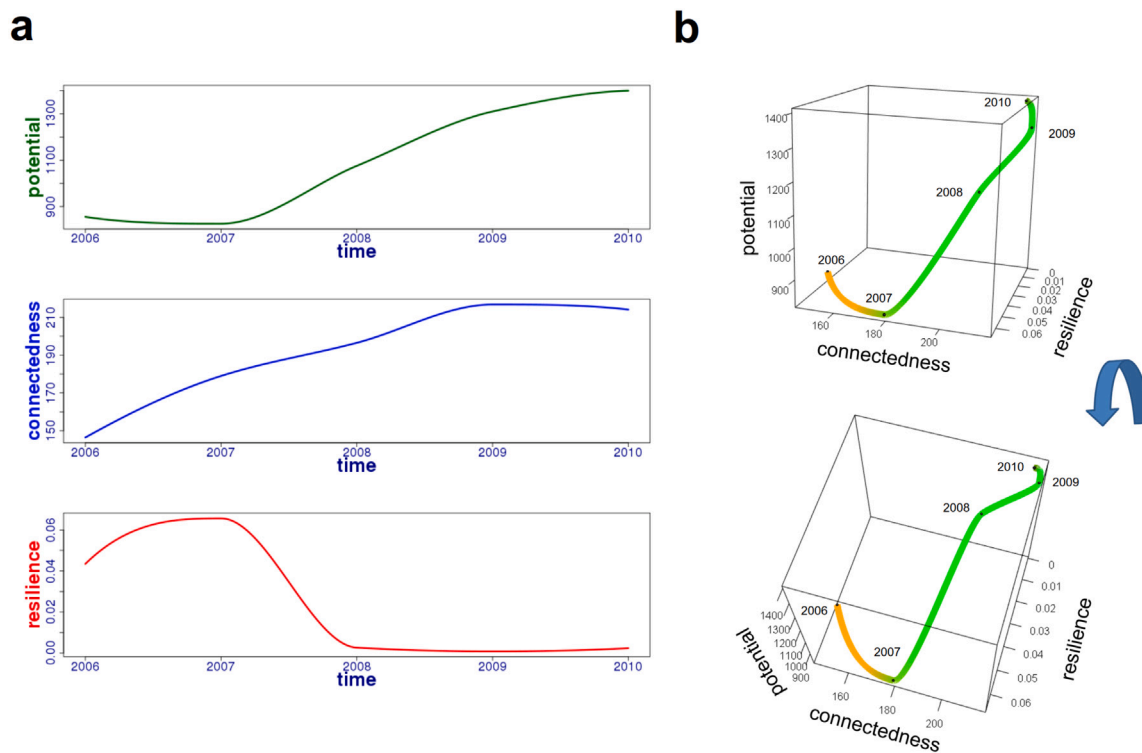


Fig. 11. Development of the three systemic variables in plot B1A22 between 2006 and 2010. (a) Potential, connectedness, and resilience of the plant community. (b) Three-dimensional plot of potential, connectedness, and resilience from two different perspectives.

In contrast to the analysis of community B4A18, we will not consider the information networks themselves but make use of the eigen-centrality heatmap shown in Fig. 9. Observe that in every year, there is a clearly outstanding subcommunity of highly central species. The

composition of this community only slightly changes during the analysis period. In order to get an insight into the functional role of the species in these central subcommunities, we consider the species-specific *in- and outflows*. By *inflow*, we denote all information being

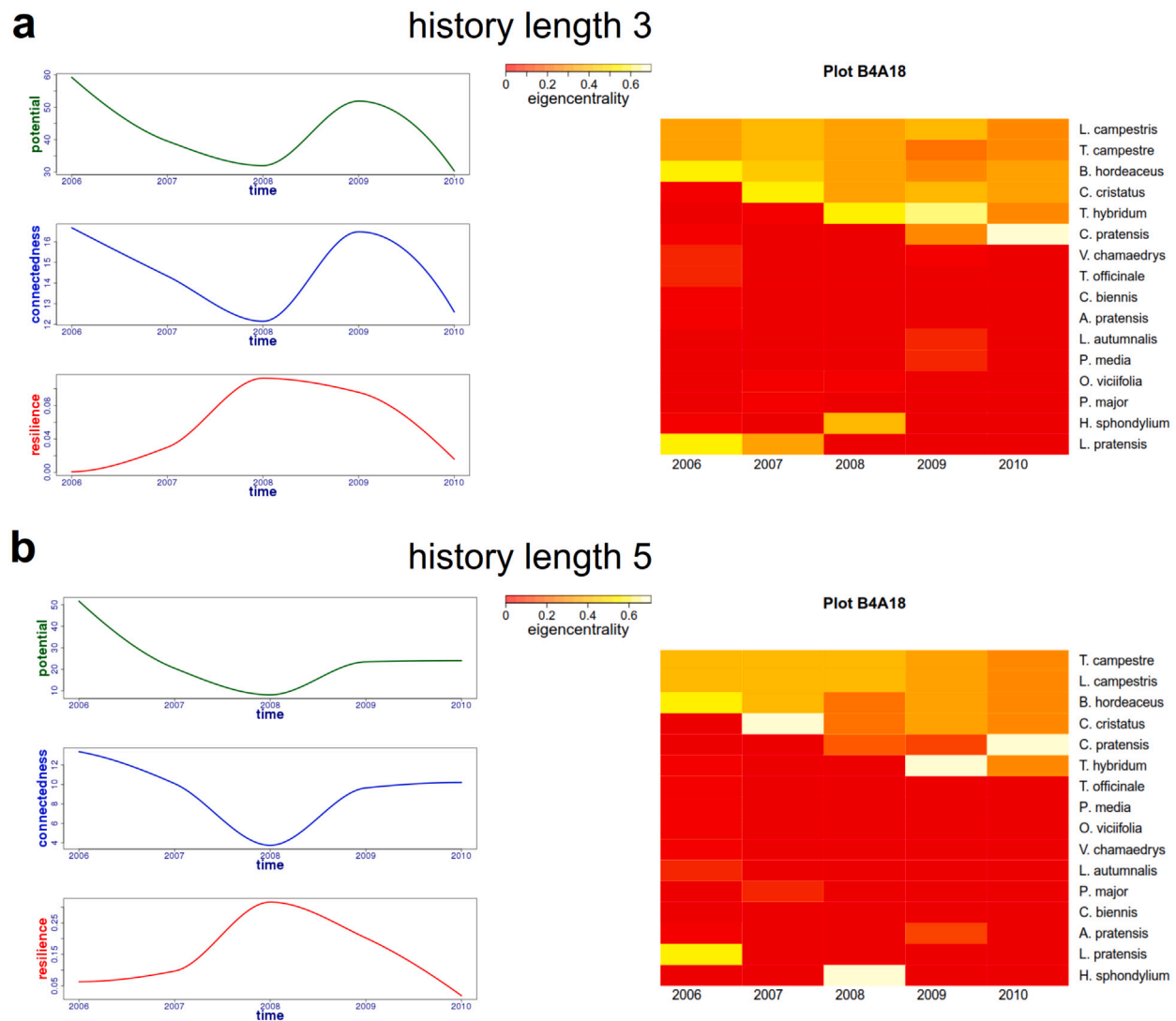


Fig. A.1. Sensitivity analysis with respect to varying history length in the case of plot B4A18. Displayed are the systemic variables and the eigencentality heatmap estimated using a history length (a) three (b) five.

transferred to the respective species. Analogously, *outflow* sums all information being transferred from the respective species to others. Simply put, the information being transferred from species A to species B at a specific time point measures the degree to which A's upcoming abundance is influenced by B's abundance. In ecological terms, such a transfer could for example reflect effective competitive, mutualistic, or commensalistic interactions among the species.

As exemplarily shown using the examples of *T. campestre*, *T. dubium*, and *T. fragiferum* (Fig. 10(a)–(c)), most central species are constant net inflowers, hence, the amount of information received and processed dominates. We interpret information processing as active adaptation of the respective component to its environment. In contrast, most species showing low centrality either do not show a clear information profile or are net outflowers, as *L. corniculatus* (Fig. 10(d)). Overall, from an information theoretic point of view, the system consists of a developing small core of 'active' species, which can be seen as key-players of the system, and a large amount of peripheral, rather 'passive' species. Interestingly, the most central species are not automatically the most abundant species.

Finally, we want to consider the development of the systemic variables of the community. Fig. 11 shows that both potential and connectedness almost monotonously increase throughout the analysis period. Resilience overall decreases. This interplay suggests that the system has been in an *r/K*-phase for the last years.

5. Conclusion

The R-package QtAC combines the analysis of component-specific behavior and emergent phenomena, thereby enabling a holistic approach to the understanding of complex systems. In the form of time-series of abundance data, only the most basic and mostly available information about a system is required. The generality of the underlying method as well as the clear workflow allow usability across the wide range of disciplines working with measurement units that are equivalent to abundance.

However, a certain background knowledge of the system and its components is necessary to make reasonable parameter choices. Besides, we recommend users to conduct a sensitivity analysis with respect to technical parameters like the amount of noise added in the estimation or the level of significance in the filtering process.

Future work is mainly going to be dedicated to customizability of the network estimation. In a very heterogeneous set of system components, component-wise choices of embedding length and embedding delay could increase preciseness of the estimations. The same applies for the parameter indicating the delay between source and destination variables. Especially in spatially ordered systems, causal delays can strongly depend on the respective pair of components.

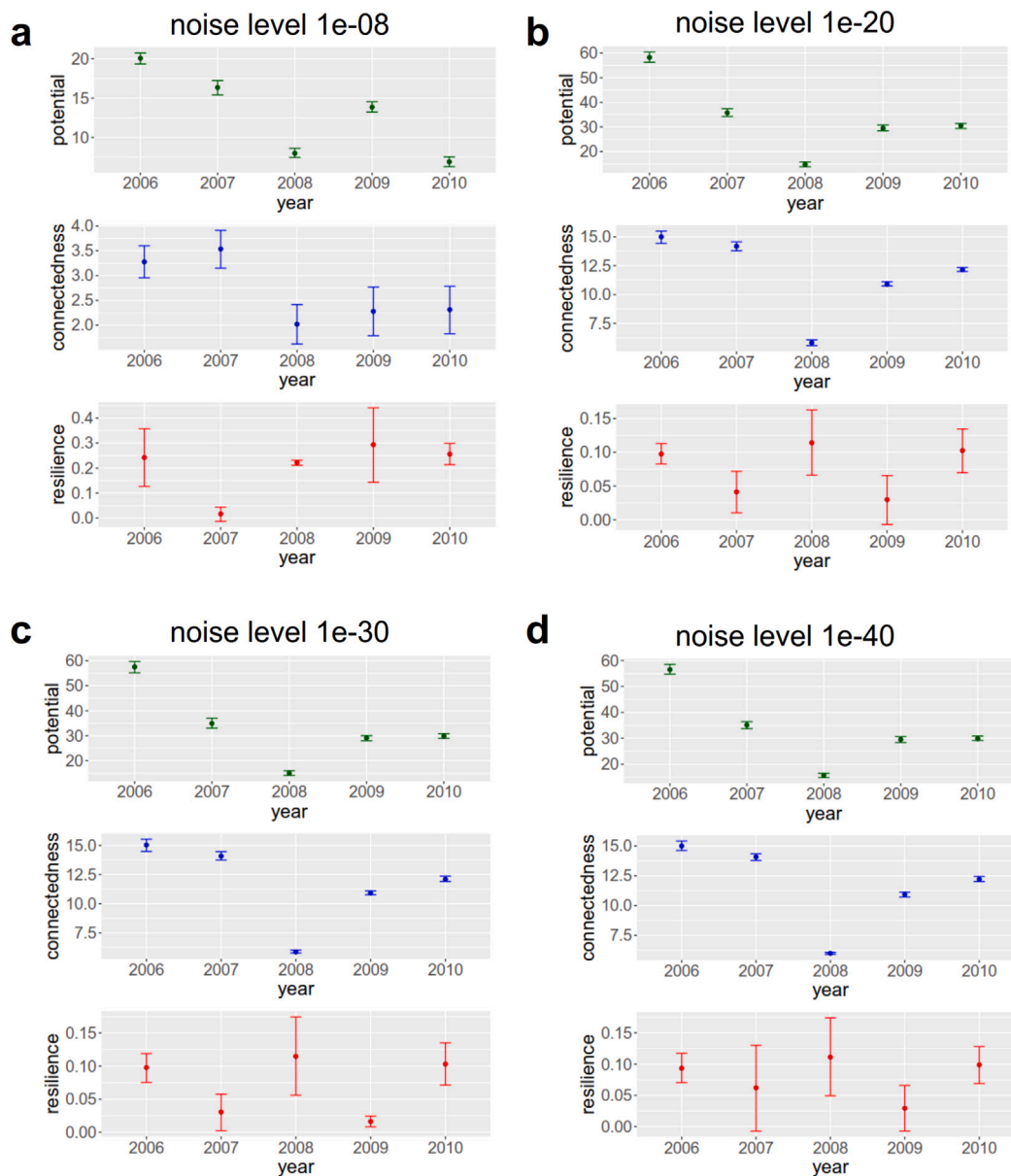


Fig. A.2. Sensitivity analysis with respect to a varying level of random Gaussian noise added in the estimation. Displayed are the systemic variables computed on basis of information networks estimated with the addition of random noise of size (a) $1e-08$ (b) $1e-20$ (c) $1e-30$ (d) $1e-40$.

In this sense, higher customizability increases the applicability of our method in spatio-temporal analysis. This branch of system analysis has steadily gained in importance throughout the last years (compare Fang et al., 2019; Islam et al., 2021; Chen and Quan, 2021 for social-ecological and economic examples). We have taken first steps into this direction analyzing flood events in a system of gauging stations in eastern Germany.

CRedit authorship contribution statement

Hannah Schrenk: Methodology, Software, Project administration, Formal analysis, Writing – original draft. **Carlos Garcia-Perez:** Software, Data curation, Visualization, Writing – review & editing. **Nico Schreiber:** Software. **Wolfgang zu Castell:** Methodology, Conceptualization, Writing – review & editing.

Declaration of competing interest

The authors declare that they have no known competing financial interests or personal relationships that could have appeared to influence the work reported in this paper.

Acknowledgment

H.S. and C. G.-P. acknowledge funding from the Initiative and Networking Fund of the Helmholtz Association through the project “Digital Earth”.

Appendix A

See Figs. A.1–A.3.

Appendix B. Data and code used in the case study

Supplementary material related to this article can be found online at <https://doi.org/10.1016/j.ecolmodel.2021.109860>.

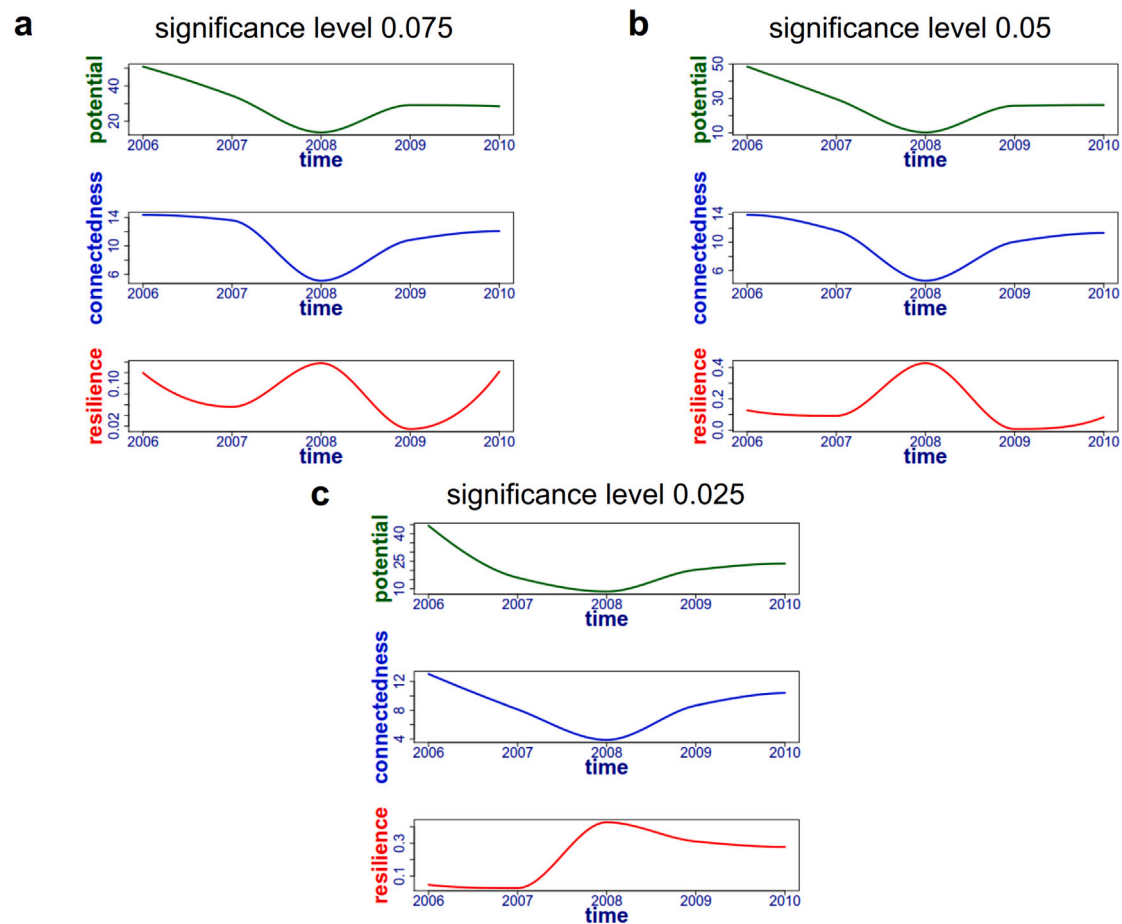


Fig. A.3. Sensitivity analysis with respect to a varying level of significance in the case of plot B4A18. Displayed are the systemic variables computed on basis of information networks filtered with respect to a significance level of (a) 0.075 (b) 0.05 (c) 0.025.

References

- Adler, D., Murdoch, D., Nenadic, O., Urbanek, S., Chen, M., Gebhardt, A., Bolker, B., Csardi, G., Strzelecki, A., Senger, A., Eddelbuettel, D., Ooms, J., Demont, Y., Ulrich, J., i Marin, X., Helffrich, G., Krylov, I., Sumner, M., the authors of shiny, the authors of knitr, the R core team, 2019. Rgl: 3D visualization using OpenGL. URL: <https://CRAN.R-project.org/package=rgl>. R package version 0.100.30.
- Allan, E., Weisser, W., Weigelt, A., Roscher, C., Fischer, M., Hillebrand, H., 2011. More diverse plant communities have higher functioning over time due to turnover in complementary dominant species. *Proc. Natl. Acad. Sci.* 108, 17034–17039.
- Allen, C., Birgé, H., Angeler, D., Arnold, T., Chaffin, B., DeCaro, D., Garmestani, A., Gunderson, L., 2018. Uncertainty and trade-offs in resilience assessments. In: *Practical Panarchy for Adaptive Water Governance: Linking Law to Social-Ecological Resilience*. pp. 243–268. http://dx.doi.org/10.1007/978-3-319-72472-0_15.
- Angeler, D., Allen, C., Garmestani, A., Gunderson, L., Hjerne, O., Winder, M., 2016. Quantifying the adaptive cycle. *PLOS ONE* 10 (12), 1–17. <http://dx.doi.org/10.1371/journal.pone.0146053>.
- Beier, C., Lovcraft, A., Chapin III, F., 2009. Growth and collapse of a resource system: An adaptive cycle of change in public lands governance and forest management in Alaska. *Ecol. Soc.* 14, <http://dx.doi.org/10.5751/ES-02955-140205>.
- Borchers, H., 2019. Pracma: Practical numerical math functions. URL: <https://CRAN.R-project.org/package=pracma>. R package version 2.2.5.
- zu Castell, W., Schrenk, H., 2020. Computing the adaptive cycle. *Sci. Rep.* 2020 (10), 18175.
- Chen, X., Quan, R., 2021. A spatiotemporal analysis of urban resilience to the COVID-19 pandemic in the Yangtze River Delta. *Nat. Hazards* 106, 1–26. <http://dx.doi.org/10.1007/s11069-020-04493-9>.
- Chung, F., 1997. Spectral Graph Theory. In: *CBMS Regional Conference Series in Mathematics*, Number 92.
- Csardi, G., Nepusz, T., 2006. The igraph software package for complex network research. *InterJ. Complex Syst.* 1695, URL: <https://igraph.org>.
- Fang, Y., Zhu, F., Yi, S., Qiu, X., Ding, Y., 2019. Role of permafrost in resilience of social-ecological system and its spatio-temporal dynamics in the source regions of Yangtze and Yellow Rivers. *J. Mt. Sci.* 16, 179–194.
- Gunderson, L., Holling, C., 2002. *Panarchy: Understanding Transformations in Human and Natural Systems*. Island Press.
- Holling, C., 1986. The resilience of terrestrial ecosystems; local surprise and global change. In: *TClark, W., Munn, R. (Eds.), Sustainable Development of the Biosphere*. Cambridge University Press, pp. 292–317.
- Islam, M.A., Paull, D.J., Griffin, A.L., Murshed, S., 2021. Spatio-temporal assessment of social resilience to tropical cyclones in coastal Bangladesh. *Geomat. Nat. Hazards Risk* 12 (1), 279–309. <http://dx.doi.org/10.1080/19475705.2020.1870169>.
- Jena Experiment, 2002. The main experiment. <http://the-jena-experiment.de/index.php/main-experiment/>. Accessed: 2021-02-06.
- Kaiser, A., Schreiber, T., 2002. Information transfer in continuous processes. *Phys. D* 166, 43–62. [http://dx.doi.org/10.1016/S0167-2789\(02\)00432-3](http://dx.doi.org/10.1016/S0167-2789(02)00432-3), 166.
- Kraskov, A., 2008. *Synchronization and Interdependence Measures and their Applications to the Electroencephalogram of Epilepsy Patients and Clustering of Data* (PhD Thesis).
- Kraskov, A., Stögbauer, H., Grassberger, P., 2004. Estimating mutual information. *Phys. Rev. E* 69 (6), <http://dx.doi.org/10.1103/PhysRevE.69.066138>.
- Lizier, J., 2014. JIDT: An information-theoretic toolkit for studying the dynamics of complex systems. *Front. Robot. AI* 1, <http://dx.doi.org/10.3389/frobt.2014.00011>.
- Marquard, E., Schmid, B., Roscher, C., De Luca, E., Nadrowski, Weisser, W., Weigelt, A., 2013. Changes in the abundance of grassland species in monocultures versus mixtures and their relation to biodiversity effects. *PLoS One* 8, e75599. <http://dx.doi.org/10.1371/journal.pone.0075599>.
- Pelling, M., Manuel-Navarrete, D., 2011. From resilience to transformation: the adaptive cycle in two mexican urban centers. *Ecol. Soc.* 16, <http://dx.doi.org/10.5751/ES-04038-160211>.
- Roscher, C., Weigelt, A., Proulx, R., Marquard, E., Schumacher, J., Weisser, W., Schmid, B., 2011. Identifying population- and community-level mechanisms of diversity-stability relationships in experimental grasslands. *J. Ecol.* 99, 1460–1469. <http://dx.doi.org/10.1111/j.1365-2745.2011.01875.x>.
- Schreiber, T., 2000. Measuring information transfer. *Phys. Rev. Lett.* 85, 461–464. <http://dx.doi.org/10.1103/PhysRevLett.85.461>.
- Schrenk, H., Betel Geijo Fernández, J., Garcia Perez, C., zu Castell, W., 2020a. Information processing in a simulated human intestinal microbiota. Preprint.
- Schrenk, H., Magnússon, B., Sigurdsson, B., zu Castell, W., 2021. Systemic analysis of a developing plant community on the island of surtsey. *Ecol. Soc.* accepted.

- Schrenk, H., Schreiber, N., Garcia-Perez, C., 2020b. QtAC (Quantifying the Adaptive Cycle). <https://github.com/hannahschrenk/QtAC>.
- Ulanowicz, R., Goerner, S., Lietaer, B., Gomez, R., 2009. Quantifying sustainability: Resilience, efficiency and the return of information theory. *Ecol. Complex.* 6, 27–36. <http://dx.doi.org/10.1016/j.ecocom.2008.10.005>.
- Vogel, A., Scherer-Lorenzen, M., Weigelt, A., 2012. Grassland resistance and resilience after drought depends on management intensity and species richness. *PLoS One* 7, e36992. <http://dx.doi.org/10.1371/journal.pone.0036992>.
- Weigelt, A., Ebeling, A., Roscher, C., Temperton, V., De Luca, E., Wagg, C., Buchmann, N., Fischer, M., Scherer-Lorenzen, M., Schmid, B., Schulze, E., Weisser, W., Luo, G., Meyer, S., 2016. Collection of aboveground community and species-specific plant biomass from the Jena Experiment (time series since 2002). <http://dx.doi.org/10.1594/PANGAEA.866358>.
- Weisser, W.W., Roscher, C., Meyer, S.T., Ebeling, A., Luo, G., Allan, E., Beßler, H., Barnard, R.L., Buchmann, N., Buscot, F., Engels, C., Fischer, C., Fischer, M., Gessler, A., Gleixner, G., Halle, S., Hildebrandt, A., Hillebrand, H., de Kroon, H., Lange, M., Leimer, S., Le Roux, X., Milcu, A., Mommer, L., Niklaus, P.A., Oelmann, Y., Proulx, R., Roy, J., Scherber, C., Scherer-Lorenzen, M., Scheu, S., Tschardt, T., Wachendorf, M., Wagg, C., Weigelt, A., Wilcke, W., Wirth, C., Schulze, E.-D., Schmid, B., Eisenhauer, N., 2017. Biodiversity effects on ecosystem functioning in a 15-year grassland experiment: Patterns, mechanisms, and open questions. *Basic Appl. Ecol.* 23, 1–73. <http://dx.doi.org/10.1016/j.baae.2017.06.002>, URL: <https://www.sciencedirect.com/science/article/pii/S1439179116300913>.